PROCEEDINGS, 45th Workshop on Geothermal Reservoir Engineering
Stanford University, Stanford, California, February 10-12, 2020
SGP-TR-216

Interpretation of In-Situ Injection Measurements at the FORGE Site

Pengju Xing[1], Duane Winkler[3], Bill Rickard[4], Ben Barker[1], Aleta Finnila[5], Ahmad Ghassemi[6], Kristine Pankow[7], Robert Podgorney[8], Joseph Moore[1], John Mclennan[2]

[1]Energy & Geoscience Institute, University of Utah, Salt Lake City, UT, USA
[2]Department of Chemical Engineering, University of Utah, Salt Lake City, UT, USA
[3]Red Rocks, Inc.
[4]Geothermal Resource Group, Palm Desert, CA, USA
[5]Golder Associates, Redmond, WA, USA
[6]Reservoir Geomechanics and Seismicity Research Group, University of Oklahoma, Norman, OK, USA
[7]University of Utah Seismograph Station, University of Utah, Salt Lake City, UT, USA
[8]Idaho National Laboratory, Idaho Falls, ID, USA

Keywords: FORGE, EGS, Injection testing, Flowback

ABSTRACT

During April and early May 2019, injection testing was carried out in three zones in a vertical well in granitic rock at the FORGE site near Milford Utah. One zone was in the uncased barefoot section in the well. Two other zones tested were cased and perforated, further uphole. One of these zones was intentionally selected because of the abundance of favorably oriented fractures (near-critically stressed) whereas the zone above it was relatively devoid of fractures. The goals of the measurement program are briefly summarized and the closure stresses determined are reported.

The results of injection-falloff and injection-flowback in each of these three zones are reported, and the implications of the measurements are described. Of particular interest are the preliminary interpretations of flowback data. Flowback offers an advantage over shut-in because of the reduced time to closure.

1. INTRODUCTION

In Sept 2017, an injection program was carried out in the openhole toe of well 58-32 at the Utah FORGE site near Milford (see, for example, Balamir et al., 2018). Well 58-32 is approximately 7500 feet deep with 147 feet of open hole below the production casing shoe. A follow-injection program was carried out in this same well in April and May, 2019. One of the aims of the 2019 testing program was to evaluate repeatability of injection into the barefoot section along with the potential for pumping into cased and perforated zones farther uphole. Post-injection measurements were undertaken under shut-in conditions or while flowing back the well. The intent of the flowback measurements was to assess previously proposed technology as a substitute for unreasonably long shut-in periods as part of Diagnostic Fracture Injection Testing.

2. OVERVIEW OF 2019 INJECTION PROGRAM

Injection was carried out in three zones in well 58-32, in April and May 2019. In each zone, a program of up to nine injection cycles was carried out. The zones are as follows.

- **Zone 1** is the barefoot section of the hole, extending from the shoe at 7348 ft MD to the plug back TD at 7525 ft MD. All depths are reported as 21.5 ft above GL to be consistent with the kelly bushing in the Sept 2017 injection program. For this zone, all gradient calculations were carried out at a depth of 7421 ft TVD RKB Sept 2017[1]. This zone had previously been stimulated in Sept. 2017, and the depth selection is consistent with the Sept 2017 campaign.
- **Zone 2** was perforated over 10 ft from 6964 to 6974 ft MD. The guns were loaded with 30-gram charges at 6 shots per foot and 60° phasing. Gradients were calculated using a true vertical depth of 6961 ft TVD RKB Sept 2017. This zone was picked because it contained an abundance of pre-existing fractures (determined from the FMI log run before casing in 2017) that were anticipated to be near critically stressed and prone to shear and dilation.
- **Zone 3** was perforated over 10 ft from 6565 to 6575 ft MD. The guns were fired at 6 shots per foot with 30-gram charges and 60° phasing. Gradients were calculated at a true vertical depth of 6562 ft TVD RKB Sept 2017. This zone contained few fractures and was labeled as the "anti-critically" stressed zone. The consequent anticipation was that breakdown would be difficult. This proved to be true.

After each zone was appropriately isolated, nine injection cycles were carried out (seven cycles in Zone 3). The goals of the injection program were as follows:

[1] For consistency with the logs run in Sept 2017, we adjust all readings in well 58-32 to the KB for the rig on location at that time (21.5 feet above ground level, GL).

- **Stimulation at higher rates than had been pumped in September 2017:** Injection was successfully performed in the April 2019 campaign, at rates up to 15 BPM. The maximum injection rate in 2017 was approximately 9 bpm. Surface pressures during pumping were completely manageable and there is still significant leeway (for higher rate injection) recognizing that the high rate injection was down 3.5-inch diameter tubing. The openhole zone (Zone 1) had been treated in Sept 2017. Bottomhole treating pressures of the cycles with comparable rates were similar this time around to those in 2019.
- **Initiation Considerations:** Perforate, breakdown, and stimulate in zones behind the casing. This was accomplished. Two cased hole zones were successfully perforated.
    a. A favorable zone for stimulation (Zone 2) was broken down and effectively stimulated with a multi-cycle program with rates up to 15 bpm.
    b. The upper zone (Zone 3), with fewer fractures and fewer favorably oriented natural fractures, was perforated. This zone could not be broken down at surface pressures up to 6500 psi. With improved isolation methods, it is anticipated that adequate pressure could be applied to break this zone down.
- **Natural Fracture Capture Potential:** Assess, if possible, the interaction with natural fractures. This can only be qualitatively inferred from the recorded microseismicity and the multiple closures that were recorded. Multiple stress levels were indicated in the pressure records suggesting access to multiple in situ fracture systems. Multiple closure signatures suggest that a diverse group of variously-oriented natural fractures, coupled with tensile features, were enfranchised in the stimulations.
- **Aseismicity:** Determine if previously stimulated zones appeared to show seismicity and what were the magnitudes. Microseismic signals were generated by the injection operations, and these were successfully recorded. There is uncertainty in the locations because of the geometrical relationship between the zones being fractured and the monitoring equipment. For Zone 1, microseismicity was generated in the openhole section where stimulation had previously been carried out. Microseismicity was also evident in Zone 2 (critically/favorably oriented natural fractures). Limited microseismicity in Zone 3 ("anti-critically/unfavorably" oriented natural fractures) was detected. This is consistent with not breaking down this zone (before failure of the isolation tools). Detectable seismicity was evident, even in the openhole zone that had been previously stimulated.
- **Additional Uphole Quantification:** Inject in two perforated zones above the barefoot section of the hole. Two zones were perforated. The lower perforated zone (Zone 2) with favorably oriented natural fractures was successfully treated. The upper perforated zone (Zone 3) was successfully perforated. Failure of isolation tools prevented significant – if any – injection into this zone. It had been intentionally selected for the anticipated difficulty in breaking it down.

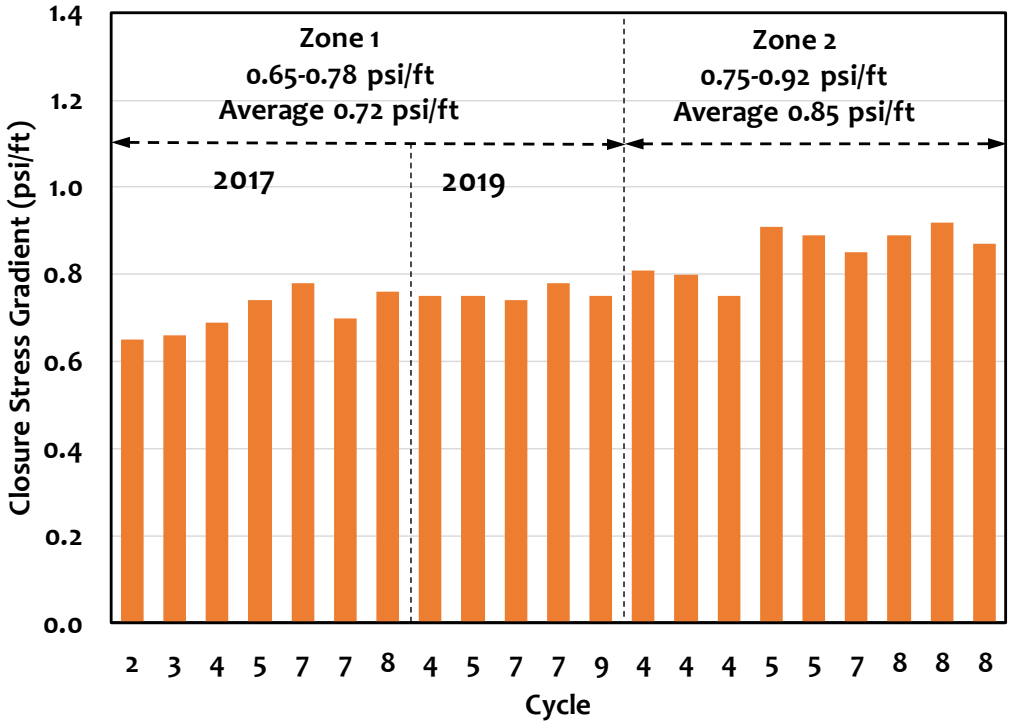

Figure 1. Compilation of reasonable stress gradients determined from multiple injection test types and interpretation methods. This plot compiles data from multiple injection cycles from two injection measurement programs (Sept 2017 and April 2019). Note each cycle may have multiple interpretations by different methods (e.g. G function, pressure vs square root of time, step rate test, log-log plot)

Tabulated stress data are included in
Figure **1**. Up to nine, relatively consistent injection-shut-in or flowback cycles were pumped in each zone. These cycles were designed to inject at different rates (from 0.4 to 15 bpm) and to carry out different injection protocols (microhydraulic fracturing, DFIT measurements, and step rate-step down testing). The 2019 injection measurements are described elsewhere (McLennan, et al., 2019; Xing et al., 2020). Three groups of stress gradients (beyond the calculated vertical stress) are evident. These are:

- Gradients in the range of 0.65 psi/ft, consistent with those seen in the September 2017 measurement program. These are either consistent with the minimum horizontal stress (particularly because of the prominence of open axial fractures in the openhole section of the well) or the pressures required for dilatancy of natural fractures. These low values could also be simply related to fracture flow rather than significant opening or reopening.
- Gradients in the range of 0.70 to 0.0.78 psi/ft, consistent with what was seen in the September 2017 measurement program. The best inference of minimum horizontal stress is in this gradient domain.
- Gradients from 0.80 to 0.92 psi/ft, were determined in the perforated zone.

The stress gradients measured in Zone 1 in 2019 are consistent with those measured in Zone 1 in 2017. In 2017 there is an increasing trend for closure with volume pumped and rate (using bottomhole data). The "apparent" stress gradients for Zone 2 (perforated) are higher than Zone 1 (openhole).

There is a wealth of pressure data available for alternative interpretations and evaluation. However, as a synopsis, several observations are reasonable.

1. The stress gradients from multiple cycles in two measurement campaigns can be interpreted to be 0.65-0.78 psi/ft in Zone 1 (measured in 2017), 0.74-0.78 psi/ft in Zone 1 (measured in 2019), and 0.75-0.92 psi/ft in Zone 2 (perforated zone, measured in 2019).
2. In 2019, some lower stress gradients were originally erroneously picked for some injection cycles. These cycles (e.g., Cycles 1-3 for Zone 1 in 2019, and Cycles 1-3 for Zone 2 in 2019) didn't open new fractures or reopen existing natural fractures.
3. There are some high apparent stress gradients (>0.90 psi/ft) inferred for Zone 2. These are attributed to dilation of natural fractures not oriented perpendicular to the minimum principal stress, as influenced by natural fractures either remote from the wellbore or as ligaments interconnecting perforations to more favorably oriented fracture systems or evolving to perpendicularity to the minimum principal stress.
4. There appears to be a rate/volume dependency indicating some degree of self-shadowing, back stress or pseudo poroelasticity.

While these observations are operationally relevant and the basic data provides excellent opportunities for assessing different procedural mechanisms for determining in situ stress (that may or may not precisely agree with those reported here), the real intent of this paper is to re-introduce the possibility of using flowback for diagnosis of closure stress and ultimately diagnosis of fracture extent and conductivity.

3. FLOWBACK FOR STRESS EVALUATION

Flowback has also being used in the petroleum sector for stress inference. Historical context for flowback measurements, from the petroleum industry, is provided in Appendix A. Flowback as a closure stress diagnostic was summarized by Plahn et al., 1995. Plahn et al. provided excerpts from relevant publications – those are reproduced here, with attribution.

Plahn et al., 1995, stated:

"The pump-in/flowback (PIFB) test is frequently used to estimate its magnitude. The test is attractive because bottomhole pressures during flowback develop a distinct and repeatable signature. This is in contrast to the pump-in/shut-in test where strong indications of fracture closure are rarely seen."

Earlier, Nolte and Smith, 1979, observed that:

"If the flow back rate is within the correct range, the resulting pressure decline will show a characteristic reversal in curvature (must be from positive to negative) at the closure pressure. The accelerated pressure decline at the curvature reversal is due to the flow restriction introduced when the fracture closes."

Shlyapobersky et al., 1988, provided a different line of reasoning that is reminiscent of the compliance method in G-function analysis:

"The distinct flowback pressure character is due to the increase of frictional pressure in the fracture and/or the decrease of fracture compliance during continuous fracture aperture reduction before the complete mechanical closure occurs. The

mechanical fracture closure is the moment at which the fracture storage, $\partial V_f/\partial p$, equals 0. Therefore, this definition of closure suggests to use the lower inflection point as an indication of mechanical closure [sic, the point at which wellbore pressure begins a more or less linear decline following the first inflection point]. At mechanical closure, the hydraulic fracture may still retain significant permeability because an incomplete hydraulic fracture closure caused by released formation particles or mismatched fracture faces. This hypothetical fracture behavior is supported by the fact that the slope of the linear pressure decline after fracture closure may be smaller than the slope estimate from the compressibility relation caused by enhanced flow from the fracture into the wellbore."

As will be seen later when actual data are provided, a shut-in following a flowback period leads to a rebound (the examples shown later have multiple flowback-shut-in cycles). Nolte, 1982, sensed the value of stabilized rebound pressures.

"The rebound pressure is the near constant pressure which occurs (following a short period of increasing pressure) after shut-in of the flowback test. This pressure is an important confirmation, provides a lower bound for the closure pressure, and is nearly equal to the closure pressure if the flowback is ended shortly after closure." (see also Soliman and Daneshy, 1991)

Other early references include Tan et al., 1988, and Hsiao et al., 1990. Like Shlyapobersky et al., 1988, Raaen et al., 2001, considered the evolution of system stiffness during flowback. "The system stiffness is the response of the well pressure due to fluid content changes resulting from leak-off to the formation or flowback at the surface. It was shown that the pump-in flowback test gives a robust and attractive method for the estimation of the minimum in-situ stress. Also, it was shown that the flowback can be performed with a constant choke rather than a constant flow rate, which simplifies test procedures." Contemporary work, Raaen and Brudy, 2001, also suggested that flowback measurements actually provide an improved (and lower) measurement of in situ stress than shut-in type measurements. A highly relevant paper, with excellent field observations and recommendations is Savitski and Dudley, 2011. In hindsight, their recommendations of reduced inflow rate are very important. In the FORGE program, the smallest available orifice was a 1/64-inch choke selection – even that may have been too aggressive, at least at early times. A consequence is decoupling of the wellbore and fracture pressures.

4. FLOWBACK AT FORGE IN APRIL 2019

Recognizing the insights of earlier researchers, it was decided to try flowing back – rather than shutting in – on some of the injection cycles that were pumped. There was some trial and error and consequently, the flowback data in all zones evaluated may not be suitable. There are some relevant data. The data and possible interpretation methods are presented to demonstrate the possible viability of this expedited measurement technique.

As with shut-in data, at a minimum (as can be seen from the historical perspective of flowback measurements presented earlier) flowback data can be used to evaluate the closure pressure and permeability (transmissibility). Five cycles in Zone 1 and five cycles in Zone 2 were operated with flowback. As indicated, not all of these data are interpretable for closure stress measurements – either because flowback was not started soon enough after shutdown or volumetric flowback rate measurements had not yet been adequately refined on location for some of the early measurements. When the flowback is started too late after shutdown, the corresponding pressure would be lower than the closure pressure, which prevents inference of the closure stress.

Flowback procedures and possible interpretations are summarized by considering three injection-flowback cycles as case studies.

4.1 Case Study 1 (Cycle 9, Zone 2)

Cycle 9 was the final injection cycle when treating Zone 2 in 2019. As was indicated, Zone 2 was perforated from 6964 to 6974 ft MD. The guns were loaded with 30-gram charges at 6 shots per foot and 60° phasing. Gradients were calculated using a true vertical depth of 6961 ft TVD RKB Sept 2017. For this injection cycle, Milford city water was pumped at 15 bpm for ~10 minutes. The well was then shut-in and the pressure dropped (refer to Figure 2). After 28 minutes of shut-in, a controlled flowback program was initiated, with cyclic flowback and shut-in as can be seen in Figure 2. About 90 bbl of fluid were recovered.

Following Savitski and Dudley, 2011, the closure pressure can be inferred from a plot of pressure vs. returned volume curve, as shown in Figure 3. The closure pressure corresponds to a deviation from linearity. From this figure, the surface pressure corresponding to apparent closure is 1500 psi and the corresponding stress gradient is 0.65 psi/ft. A hydrostatic gradient of 0.433 psi/ft is assumed and the total hydrostatic pressure is calculated to be 3014 psi.

Based on the legacy of interpretation methods for interpreting flowback in the petroleum industry, a plot of reciprocal productivity index vs square root of material balance time is also suggested as a method to infer the closure stress from a flowback procedure. The reciprocal productivity index, RPI, is $(p_i - p_w)/q$, where p_i is the initial pressure, p_w is the wellbore pressure and q is the flowback rate. The material balance time (Palacio and Blasingame, 1993) is defined as:

$$t_{mb}(t_x) = \frac{Q(t_x)}{q(t_x)} \tag{1}$$

where $Q(t_x)$ is the cumulative recovered volume at time t_x, and $q(t_x)$ is the flowback rate at t_x. The reciprocal productivity index (RPI) versus square root of material balance time for Zone 2, Cycle 9 is shown in Figure 4. As can be seen in the figure, the green circle represents the end of a linear trend, which suggests a stress gradient of 0.64 psi/ft. This is close to the result obtained from the method in Figure 3.

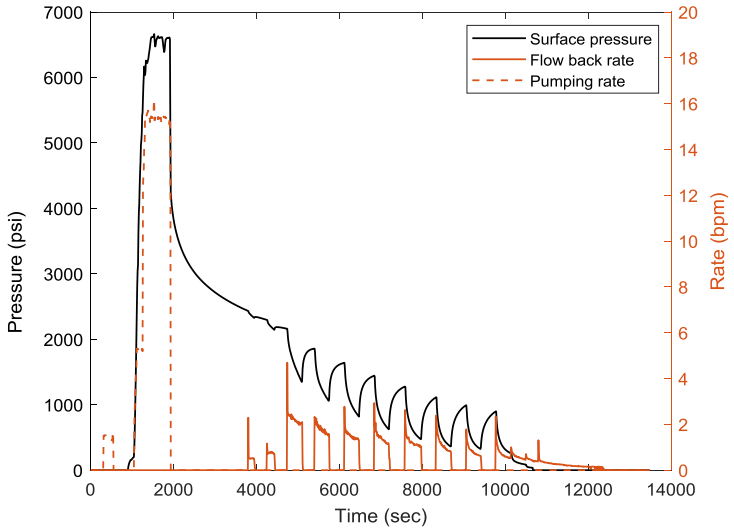

Figure 2. Injection and flowback data for Zone 2, Cycle 9. The flowback involved opening the choke for a prescribed period of time and then shutting in and repeating this until the pressure was bled down. In hindsight, smaller duration opening/closing cycles are recommended. The flowback rate was measured. No temperature corrections were applied.

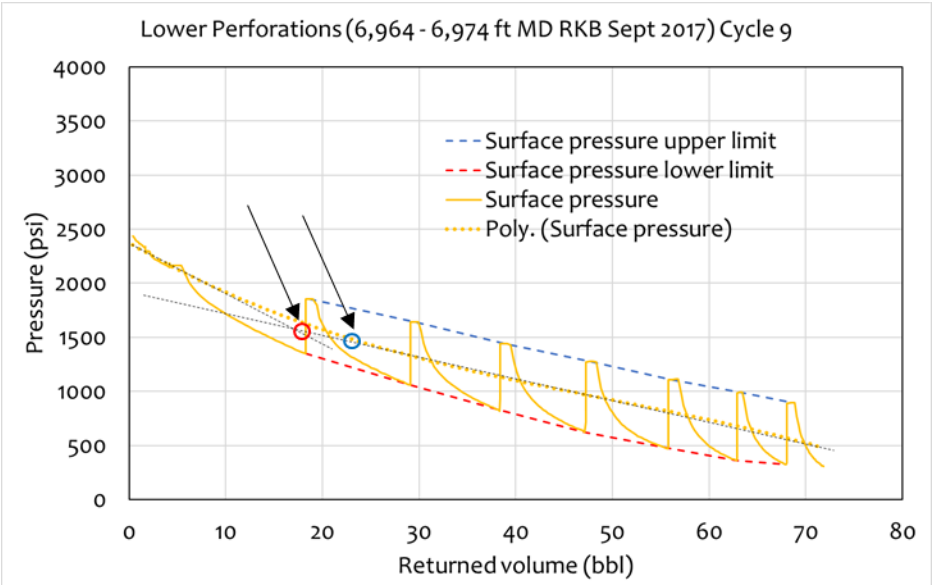

Figure 3. Surface pressure vs. returned volume for Zone 2, Cycle 9. The surface pressure at closure is around 1500 psi and the stress gradient is 0.65 psi/ft, given the point (blue circle) deviating from the linear line is chosen. If the intersection point (red circle) of the two linear section is chosen, the surface pressure at closure is 1600 psi and the stress gradient is 0.66 psi/ft. Learnings include starting the flowback immediately following shutdown and using shorter shut-in-flowback cycles. This ensures not missing early closure and having a more definitive plot of pressure versus returned volume.

The flowback data can also be used to calculate transmissibility using multi-rate superposition concepts. Figure 5 shows a two-rate example taken from the flowback period for Zone 2, Cycle 9. The slope m can be obtained from a plot of pressure p_w vs. $\log\frac{t+\Delta t\prime}{\Delta t\prime}+\frac{q_2}{q_1}\log\Delta t'$ (see Figure 6). Here q_1 is the pressure prior to rate change, q_2 is the rate after rate change, t is the time duration of q_1, and $\Delta t'$ is the time measured from the instant of the rate change. The transmissibility can be calculated as (Equation 6.9 in Matthews and Russell, 1967):

$$kh=\frac{162.6\,q_1\mu B}{m}=\frac{162.6\times 2505.6\times 0.25\times 1.0}{691}=101.6\ \text{md}\cdot\text{ft} \tag{2}$$

In Equation (2), the units for the flow back rate, q_1, are bpd. B is the formation volume factor and is taken as 1.0. The viscosity μ is approximated as 0.25 cP at 300°F and 4000 psi. This method offers potential and can presumably be refined by considering partial completion skin and fracture skin effects.

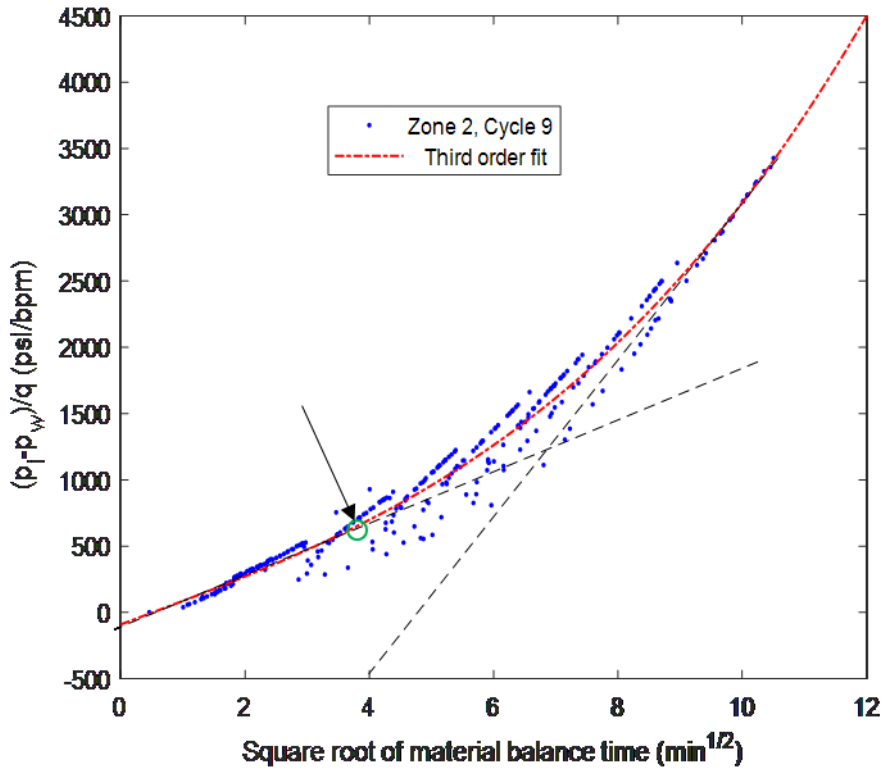

Figure 4. Reciprocal productivity vs. square root of material balance time of Zone 2, Cycle 9. The red dash dotted line represents a third order fit of the data. Taking a point (green circle) as the end of the first linear trend, the pressure drop at apparent closure is 1028 psi. The inferred surface pressure is 2435-1028=1407 psi. The corresponding closure pressure is 1407+3014=4421 psi and the stress gradient is 0.64 psi/ft.

It is also possible to do a multiple cycle analysis to obtain the transmissibility using a cross plot of $(p_i-p_w)/q_n$ and the Odeh-Jones time function (Odeh and Jones, 1965):

$$T=\sum_{i=1}^{n}\frac{q_i-q_{i-1}}{q_n}\log(t_n-t_{i-1}) \tag{3}$$

where q_i is the flowback rate for the ith step, and t_i is the time of the ith step rate since the initiation of flowback. However, in this case, there were shut-in periods between each flowback rate, which makes both the RPI and the Odeh-Jones time infinite. Hence, a very small flowback rate is assumed during the shut-in period. Figure 7 demonstrates a multiple rate analysis of this sort for Zone 2, Cycle 9 (see Figure 2). The slope of the multiple rate analysis is obtained as $m=0.33$ from Figure 8. The transmissibility can be calculated as:

$$kh=\frac{70.6\,\mu B}{m}=\frac{70.6\times 0.25\times 1.0}{0.33}=53.6\ \text{md}\cdot\text{ft} \tag{4}$$

The formation volume factor is also taken as 1.0 here. This calculated transmissibility value is smaller than that calculated using Matthew and Russell's two-rate method. This could be due to the difficulties of handling the shut-in period in multiple rates method.

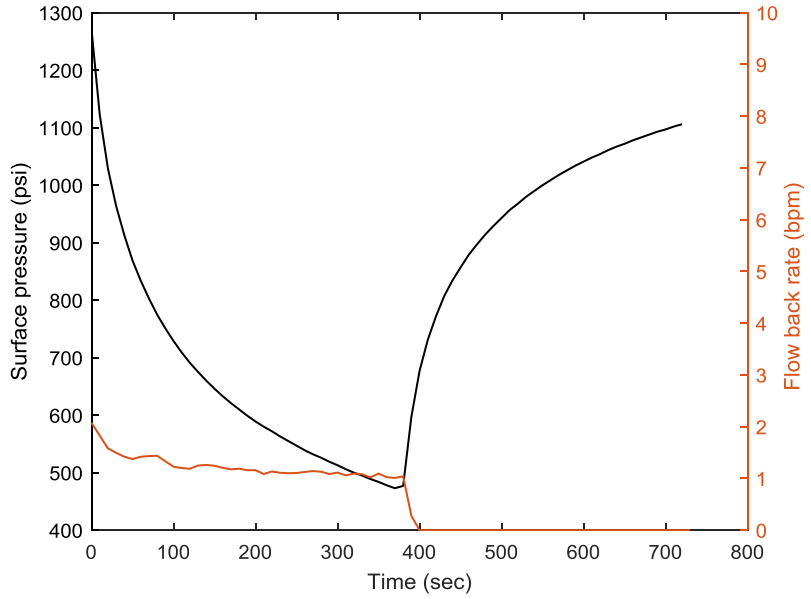

Figure 5. Two rate analysis plot (flowback and shut-in), taken from the 7590-8310 sec cycle for Zone 2, Cycle 9. The first flow back rate q_1 is 1.2 bpm and the second flow back rate q_2 is 0.0 bpm. Surface pressure is shown in black and the flowback rate is shown in red.

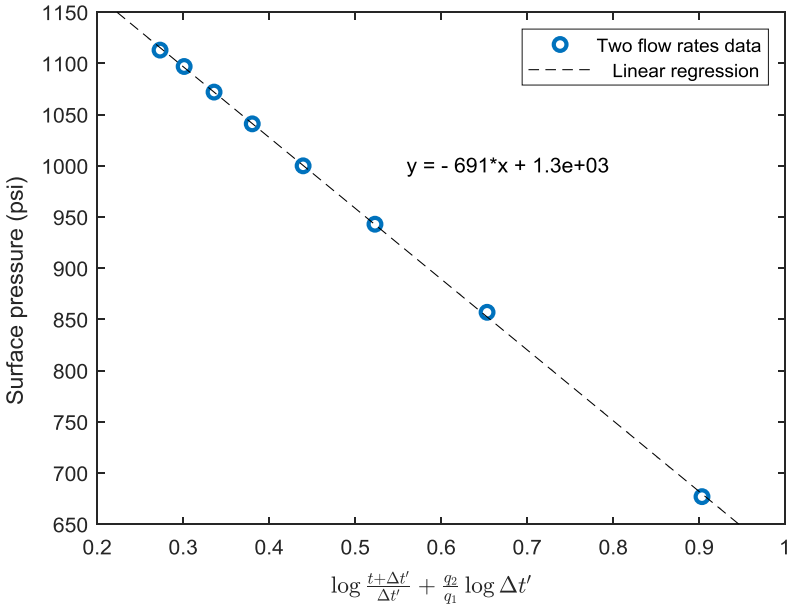

Figure 6. Pressure vs. $\log \frac{t+\Delta t'}{\Delta t'} + \frac{q_2}{q_1} \log \Delta t'$ for the two flow rate tests. The slope m is 691 psi. Several representative data points from Figure 5 are used to construct this plot. q_1, the pressure prior to rate change, equals 1.2 bpm, and q_2 is 0 bpm.

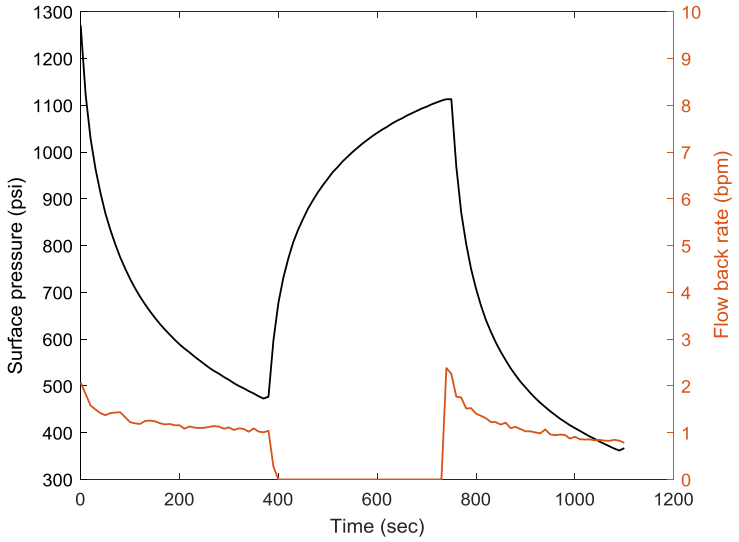

Figure 7. Multiple flow rate test plot, taken from the 7590-8690 sec sequence of Zone 2, Cycle 9. The first flowback rate q_1 is 1.2 bpm and the second flowback rate q_2 is 0.0 bpm and the third flowback rate q_3 is 1.06 bpm.

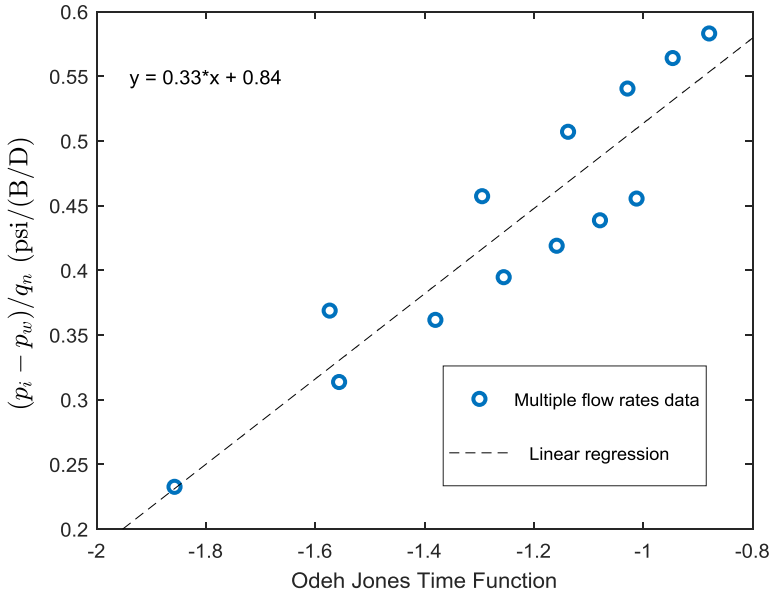

Figure 8. RPI vs Odeh-Jones time for the multiple rate tests. The slope *m* is used to infer the transmissibility in a conventional radial flow relationship.

4.2 Case Study 2 (Cycle 7, Zone 2)

Cycle 7 was a step rate/step down cycle applied to Zone 2 in 2019. As indicated for the previous case, Zone 2 was perforated from 6964 to 6974 ft MD. The guns were loaded with 30-gram charges at 6 shots per foot and 60° phasing. Gradients were calculated using a true vertical depth of 6961 ft TVD RKB Sept 2017.

In Cycle 7, 190 bbl were pumped. After shut-in for 19 minutes, flowback started through a 1/64-inch choke. The choke was beaned up in 1/64-inch increments from 1/64-inch to 4/64-inch. After 105 bbl fluid were recovered, the flow was too small to measure. The pressure and rate data are shown in Figure 9.

As in the previous demonstration, RPI is plotted versus the square root of material balance time for Zone 2, Cycle 7 (refer to Figure 10.). The inferred stress gradient (0.68 psi/ft) is close to that of in Case Study 1 for Zone 2, Cycle 9.

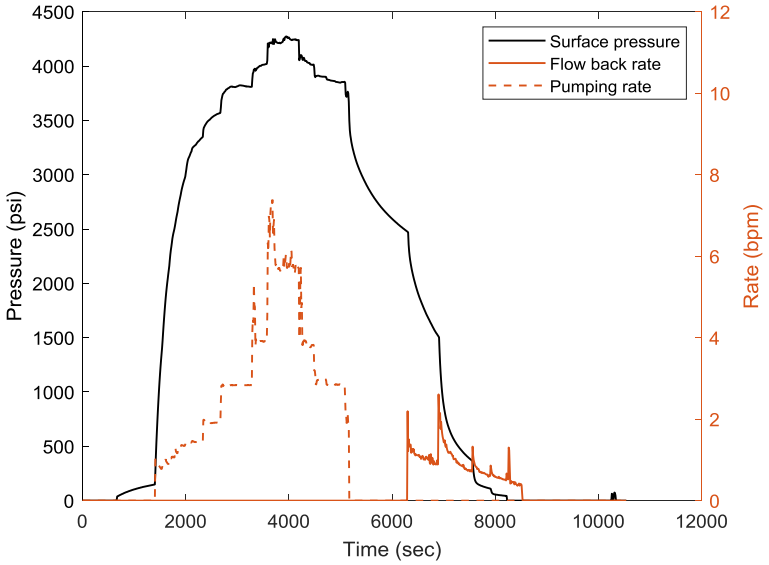

Figure 9. Injection and flowback data for Zone 2, Cycle 7. The flowback was initiated after 19 minutes shut-in.

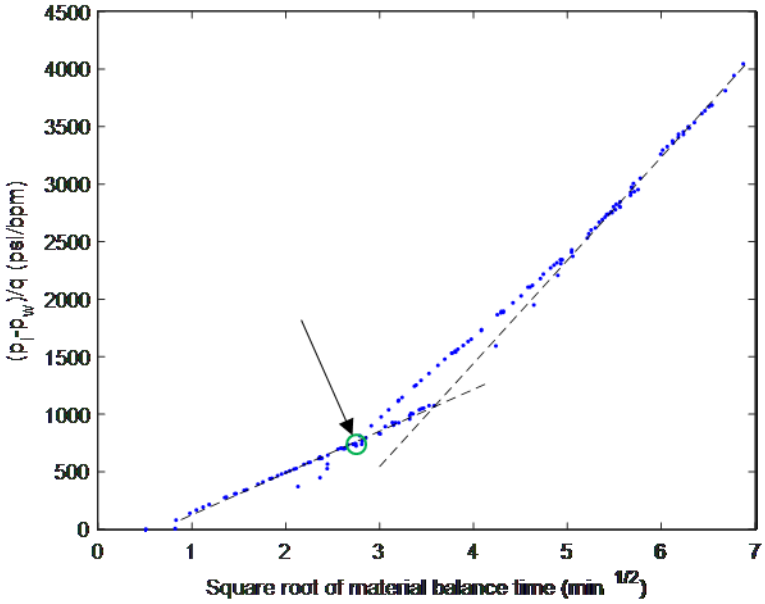

Figure 10. Reciprocal productivity vs. the square root of material balance time for Zone 2, Cycle 7. At the point of deviation from the first linear section (green circle), the pressure drop is 758 psi. Using this as a possible diagnostic, the inferred surface pressure at closure is 2478-758=1720 psi. The corresponding closure pressure is 1720+3014=4734 psi and the associated stress gradient is 0.68 psi/ft.

4.3 Case Study 3 (Cycle 5, Zone 2)

In this case, Cycle 5 injection into Zone 2, the treatment entailed pumping Milford city water at ~5 bpm for ~5 minutes; 33 bbl fluid were pumped. After a ten-minute shut-in, the well was flowed back through a 1/64-inch choke. After one hour, the flowback rate was too small to measure. A total of 17.6 bbl were recovered (Figure 11).

As in Case Study 1 and Case Study 2, a plot of RPI versus the square root of material balance time was used to infer the closure pressure (see Figure 12). The calculated stress gradient is 0.62 psi/ft.

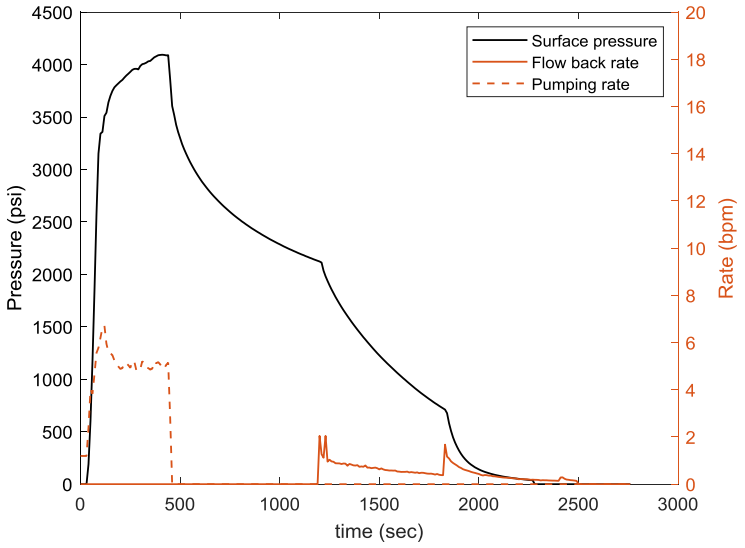

Figure 11. Injection and flowback data for Zone 2, Cycle 5. The flowback was initiated after 10 minutes of shut-in.

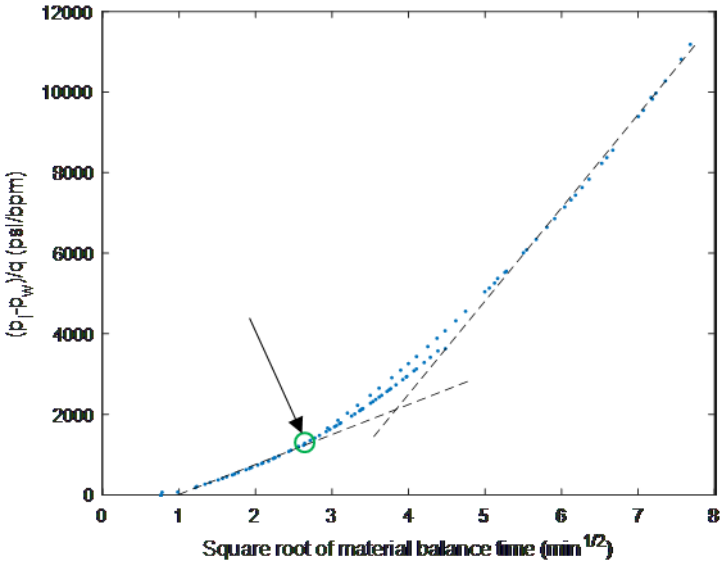

Figure 12. Reciprocal productivity vs. the square root of material balance time for Zone 2, Cycle 5. The pressure drop is 811 psi (green circle). Then the surface closure pressure is 2123-811=1312 psi. The stress gradient is 0.62 psi/ft.

This is a good case for comparison with shut-in data.
Figure13 shows the pressure-time data for Zone 2, Cycle 4, April 2019. Conventional closure stress gradient interpretation from that information suggests a gradient of 0.80 psi/ft (Figure 13). The gradient from shut-in is substantially higher than for flowback. This could suggest that, when analyzing flowback data (Figure 12 for example) an artificial gradient is being picked due to the fact that the flowback started late, or 2) flowback offers a very useful method for closure stress interpretation in naturally fractured reservoirs where there is awkward communication between the wellbore and a natural fracture system. In the first case, it is possible that the flowback was not started soon enough in the case studies presented. If that is the case, the closure point picked from a pressure vs. returned volume curve or the RPI vs. the square root of the material balance time may not adequately represent the whole trend. This could result in an underestimation of the closure stress. There will be future research work to clarify this.

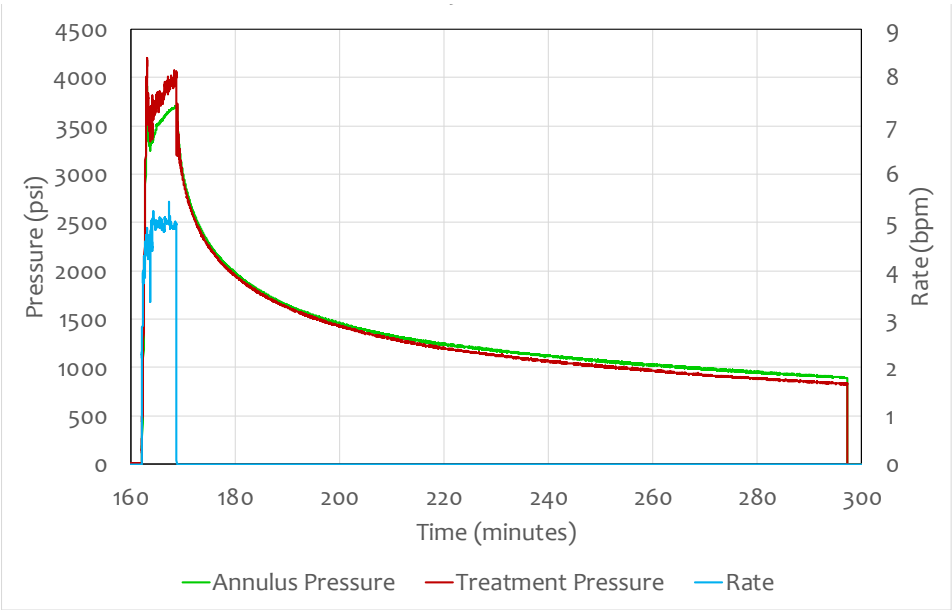

Figure13. Pressure and rate data for the injection cycle immediately preceding the injection shown for Zone 2 Cycle 5 in Figure 11. This cycle (Zone 2 Cycle 4) was shut-in for an extended period of time.

5. CONCLUSIONS

Several cases with flowback were analyzed from treatments in Zone 2 of Well 58-32. The horizontal minimum stress gradient inferred ranged from 0.62-0.68 psi/ft. These stress gradients are smaller than values from the extended shut-in analysis (e.g., G function interpretations). There may be alternative interpretations if the flowback had been started earlier. Regardless, flowback seems to be a promising methodology with significant operational advantages in terms of rig time.

The measurements are slightly more complicated than simple shut-ins because some form of flowback rate continuous recording is necessary. Flowback was recorded in Zone 2 with a turbine meter. The data recorded in Zone 1 with a stopwatch a five-gallon bucket were inadequate. Lessons learned were that smaller duration flowback-shut-in cycles could be desirable and that it may be prudent to start flowback as soon as feasible after shutdown. The transmissibility obtained from the flowback data is about 100 md·ft, which is consistent with transmissibility inferred using after closure analysis following conventional DFIT shut-in practices.

ACKNOWLEDGEMENTS

Funding for this work was provided by the U.S. DOE under grant DE-EE0007080 “Enhanced Geothermal System Concept Testing and Development at the Milford City, Utah FORGE Site.” We thank the many stakeholders who are supporting this project, including Smithfield, Utah School and Institutional Trust Lands Administration, and Beaver County as well as the Utah Governor’s Office of Energy Development.

REFERENCES

Abbasi, M.A., Dehghanpour, H. and Hawkes, R.V. 2012. Flowback Analysis for Fracture Characterization, SPE 162661, SPE Canadian Unconventional Resources Conf., Calgary, AB, 30 Oct. - 1 Nov.

Al-Ali, A.H., Al-Anazi, H.A., Abdul Aziz, A., Panda, S.K., Al-Hajji, A.A. 2016. Optimization of Post-Hydraulic Fracturing Flowback Cleanup Utilizing Polymer Content Determination in Flowback Liquid Samples, SPE 180083, SPE Europec, 78th EAGE Conf. Exhib., Vienna, Austria, 30 May – 2 June.

Al-Saihati, A.H., El Hajj, H., Ortiz, R., Bittar, M., and Shakeel, M. 2015. Fracture Cleanup Determination by Guar Measurement in Flowback Water Samples, SPE 172560, SPE Middle East Oil & Gas Show and Conf., Manama, Bahrain, 8-11 March.

Asadi, M., Woodroof, R.W., Malone, W.S., and Shaw, D.R. 2002. Monitoring Fracturing Fluid Flowback With Chemical Tracers: A Field Case Study, SPE-77750-MSSPE Annual Technical Conference and Exhibition, 29 September-2 October, San Antonio, TX.

Balamir, O., Rivas, E., Rickard, W. M., McLennan, J., Mann, M., and Moore, J. 2018. Utah FORGE Reservoir: Drilling Results of Deep Characterization and Monitoring Well 58-32. In Proc. 43rd Workshop on Geothermal Reservoir Engineering, Stanford University, Stanford, California.

Bertoncello, A., Wallace, J. Blyton, C., Honarpour, M., and Kabir, C.S. 2014. Imbibition and Water Blockage in Unconventional Reservoirs: Well management Implications During Flowback and Early Production, SPE 167698, SPE/EAGE European Unconventional Conf. and Exhib., Vienna, Austria, 25-27 Feb.

Clarkson, C.R. 2012. Modeling 2-Phase Flowback of Multi-Fractured Horizontal Wells Completed in Shale, SPE 162593, SPE Canadian Unconventional Resources Conf., Calgary, AB, 30 Oct. - 1 Nov.

Crafton, J.W. 1998. Well Evaluation Using Early Time Post-Stimulation Flowback Data, SPE ATCE, New Orleans, LA, September 27-30.

Crafton, J.W. 2008. Modeling Flowback Behavior or Flowback Equals “Slowback”, SPE 119894, SPE Shale Gas Production Conf., Fort Worth, TX November.

Crafton, J. 2010. Flowback Performance in Intensely Naturally Fractured Shale Gas Reservoirs, SPE 131785, SPE Unconventional Gas Conf., Pittsburgh, PA, 23-25 February.

Deen, T., Daal, J., and Tucker, J. 2015. Maximizing Well Deliverability in the Eagle Ford Shale Through Flowback Operations, SPE 174831, SPE ATCE, September 28-30.

Fei, W., Ziqing, P., Hun, L., and Shicheng, Z. 2016. A Chemical Potential Dominated Model for Fracturing-Fluid Flowback Simulation in Hydraulically Fractured Shale, SPE 181418, SPE ATCE, Dubai, UAE, 26-28 September.

Gdanski, R., Weaver, J., and Slabaugh, B. 2007. A New Model for Matching Fluid Flowback Composition, SPE Hydraulic Fracturing Tech. Conf., College Station, TX, January 29-31.

Ghahri, P., Jamiolahmady, M., Soharbi, M. 2011. A Thorough Investigation of Cleanup Efficiency of Hydraulic Fractured Wells Using Response Surface Methodology, SPE 144114, European Formation Damage Conf., Noodwijk, The Netherlands, 7-10 June

Hsiao, C., and Tsay, F.S. 1990. Evaluation of Fracture Parameters Using Pump-ln/Flowback Test, CIM/SPE 90-3, 1990 CIM/SPE International Technical Meeting, Calgary, June 10-13.

Ilk, D., Currie, S.M., Simmons, D., Rushing, J.A., Broussard, N.J., and Blasingame, T.A. 2010, A Comprehensive Workflow for Early Analysis and Interpretation of Flowback Data from Wells in Tight Gas/Shale Reservoir Systems, SPE ATCE, Florence, Italy, 19-22 September.

Matthews, C.S., and Russell, D.G. 1967. Pressure Buildup and Flow Tests in Wells, SPE Monograph Series Vol. 1, ISBN: 978-0-89520-200-0, Society of Petroleum Engineers.

McLennan, J.D., Moore, J. 2019. Utah FORGE: Phase 2C Topical Report, Appendix A Injection Measurements in Well 58-32 (April and May 2019).

Nolte, K.G. 1982. Fracture Design Considerations Based on Pressure Analysis, SPE 10911, 1982 SPE Cotton Valley Symposium, Tyler, TX, May 20.

Nolte, K.G. and Smith, M.B. 1979. Interpretation of Fracturing Pressures," JPT (Sept. 1981) 1767-75.

Odeh, A.S. and Jones, L.G. 1965. Pressure Drawdown Analysis, Variable-Rate Case, SPE-1084, JPT, Vo. 17, Issue 8, August.

Palacio, J.C., and Blasingame, T.A. 1993. Decline Curve Analysis Using Type Curves – Analysis of Gas Well Production Data, SPE 25909, Joint Rocky Mountain Regional and Low Permeability Reservoirs Symp., 26-28 April.

Plahn, S.V., Nolte, K.G. and Miska, S. 1995. A Quantitative Investigation of the Fracture Pump-In/Flowback Test, SPE 30504, SPE ATCE, Dallas, TX, 22-25 October.

Pope, D., Britt, L., Constien, V., Anderson, A., and Leung, L. 1995. Field Study of Guar Removal from Hydraulic Fractures, SPE 31094, 1995 Intl. Symp. on Formation Damage Control, Lafayette, LA, 14-15 February.

Raaen, A.M., and Brudy, M., 2001. Pump-in/Flowback Tests Reduce the Estimate of Horizontal in-Situ Stress Significantly, SPE 71367, SPE Annual Technical Conference and Exhibition held in New Orleans, Louisiana, 30 September–3 October.

Raaen, A.M., Skomedal, E., Kjørholt, H., Markestad, P., and Økland, D. 2001. Stress Determination from Hydraulic Fracturing Tests: The System Stiffness Approach”. Int. J. Rock Mech. Min. Sci., 38 (4), 531–543

Rose, P. 2017. The Use of Amino-Substituted Naphthalene Sulfonates as Tracers in Geothermal Reservoirs", Proceedings 42nd Workshop on Geothermal Engineering, Stanford University. Published, 02/13/2017.

Rose, P. 2017. Tracer Testing to Characterize Hydraulic Stimulation Experiments at the Raft River EGS Demonstration Site. GRC Transactions, 05/17/2017.

Savitski, A., and Dudley, J.W. 2011. Revisiting Microfrac In-situ Stress Measurement via Flow Back - A New Protocol, SPE-147248, SPE Annual Technical Conference and Exhibition, 30 October-2 November, Denver, CO.

Shlyapobersky, J., Walhaug, W.W., Sheffield, R.E., and Huckabee, P.T. 1988. Field Determination of Fracturing Parameters for Overpressure Calibrated Design of Hydraulic Fracturing," SPE 18195, 1988 SPE Annual Technical Conference and Exhibition, Houston, Oct. 2-5.

Soliman, M.Y., and Daneshy, A.A. 1991. Determination of Fracture Volume and Closure Pressure from Pumpln/ Flowback Tests, SPE 21400, 1991 SPE Middle East Oil Show, Bahrain, Nov. 16-19.

Tan, H.C., McGowen, J.M., Lee, W.S., and Soliman, M. Y .1988. Field Application of Minifracture Analysis to Improve Fracturing Treatment Design, SPE 17463, 1988 SPE California Regional Meeting, Long Beach, March 23-25.

Valenzuela Munoz, A., Asadi, M., Woodroof, R.A., and Rogelio Morales, R. 2009. Long-Term Post-Frac Performance Analysis Based on Flowback Analysis Using Chemical Frac-Tracers, SPE-121380, Latin American and Caribbean Petroleum Engineering Conference, 31 May-3 June, Cartagena de Indias, Colombia.

Vazquez, O., Mehta, R., Mackay, E., Linares-Samaniego, S., Jordan, M., and Fidoe, J. 2014., Post-frac Flowback Water Chemistry Matching in a Shale Development, SPE 169799, SPE Intl. Oilfield Scale Conf. and Exhib., Aberdeen, Scotland, UK, May 14-15.

Willberg, D.M., Steinsberger, N., Hoover, R., Card, R.J., and Queen, J. 1988. Optimization of Fracture Cleanup Using Flowback Analysis, SPE 39920, 1998 SPE Rocky Mountain Regional/Low Permeability Reservoirs Symposium and Exhibition, Denver, CO, 5–8 April.

Williams-Kovacs, J.D., Clarkson, C.R., and Zanganeh, B. 2015. Case Studies in Quantitative Flowback Analysis, SPE 175983, SPE-CSUR Unconventional Resources Conf. – Canada, Calgary, AB, 20-22 Oct.

Xu, Y., Adefidipe, O.A., Dehghanpour, H., and Virues, C.J. 2015. Volumetric Analysis of Two-Phase Flowback Data for Fracture Characterization, SPE Western Regional Meeting, Garden Grove, CA, 27-30 April.

Xing, P., Moore, J., and McLennan, J.D. 2020. Re-interpretation of Injection Data from April and May 2019: Utah FORGE, Well 2020, Report to DOE, in preparation

Yang, B.H. and Flippen, M.C. 1997. Improved Flowback Analysis to Assess Polymer Damage, SPE 38305, 1997 Production Operations Symp., Oklahoma City, 9-11 March.

Zhou, Q., Dilmore, R., Kleit, A., and Wang, J.Y. 2015. Evaluating Fracturing Fluid Flowback in Marcellus using Data Mining Technologies, SPE 173364, SPE Hydraulic Fracturing Technology, Conf. The Woodlands, TX, 3-5 February

Zolfaghari, A., Dehghanpour, H., Ghanbari, E., and Bearinger, D. 2016. Fracture Characterization Using Flowback Salt-Concentration Transient, SPE 198598, SPEJ, February.

APPENDIX A. BACKGROUND ON FLOWBACK

What Can We Learn from the Petroleum Industry?

Flowback can be considered to be the intentional sporadic or continuous recovery of fluids after treated zones are free to expel treatment and reservoir fluids to the surface – after plugs are drilled out, after swabbing, after beaning up, etc. In the geothermal sphere, opportunities for developing flowback technology include providing an alternative mechanism for assessing in situ stresses, system transmissibility, and an index for evaluating fracture surface area and fracture complexity.

Twenty-five years ago in the petroleum industry, quantifying flowback was mostly done to assess residual polymer damage and the associated degradation of conductivity (Pope et al., 1995; Yang et al., 1997; Willberg et al., 1998; Ghahri et al., 2011, Al-Ali et al., 2016; Al-Saihati et al., 2015). Historically, in hydrocarbon scenarios, operators were also concerned about flowing back more than fluid – proppant. Numerous techniques, such as forced closure, were considered to ensure near-wellbore conductivity. Concern about flowback (or overdisplacement) leading to choke skin have led to shut-in schemes ranging from the most aggressive (forced closure) to sometimes finding favorable results with prolonged shut-ins while treatments are continued and plugs are drilled out. A topical recent example to understand this has been data mining work by Zhou et al., 2015.

With time, the sophistication of flowback analysis in the petroleum industry increased. Figure A-1 is an example of flowback from a single stage in a vertical well, where particular proppant concentrations were specifically tagged with different tracers. The motivation remained understanding created surface area. The two examples demonstrate that even when completing a single zone, flowback is complicated. One figure shows FILO (first in-last out). The second shows that flow pathways can change during pumping and the last material pumped is not necessarily the first returned to the wellbore during flowback. This becomes even more important in a more modern context – and relevant to enhanced geothermal - when considering multistage generation of transverse fractures, and understanding flow partitioning in these discrete fractures. The long history of tracers in geothermal applications has been adopted by the petroleum industry (Rose, 2017a, 2017b) for evaluating partitioning of fluid in different fracturing stages in multistage horizontal completions. There is direct applicability for future activities at FORGE.

The next entrepreneurial scientific approach in flowback testing was to use reactive transport modeling to rationalize high salt concentrations encountered in some produced water scenarios. These flowback waters tend to contain a high proportion of TDS (total dissolved solids) along with other reservoir constituents.

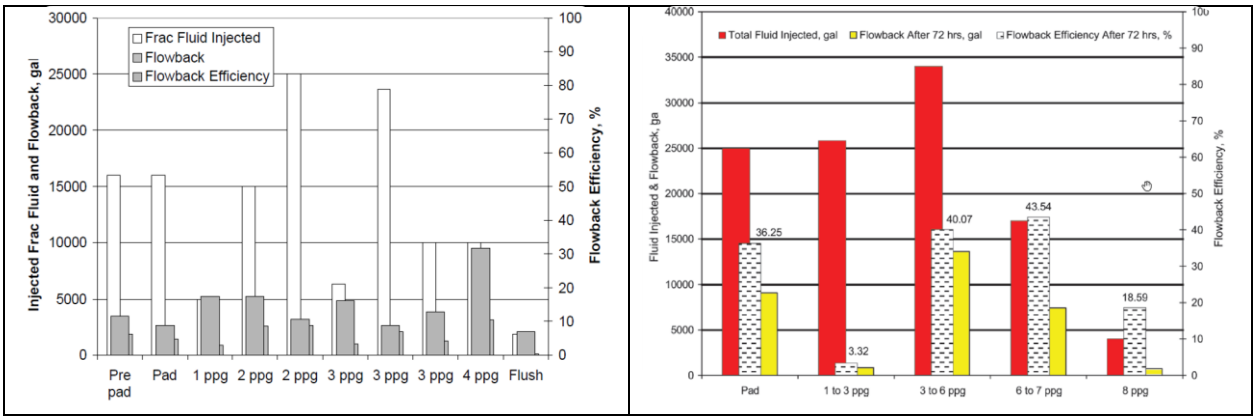

Figure A-1. At left is an example of the increasingly frequent use of tracers, delineating recovery from individual stages of a single treatment in a vertical well (Asadi et al., 2002, SPE 77750). Notice that the tracer indicated predominant load (injected fluid) recovery from the final proppant stage (vertical well). At right, are data from Valenzuela-Munoz et al., 2009 (SPE 121380). In this case, the recovery in this moderately high proppant concentration treatment was highest for the middle sand stages suggesting either override by the tail-in sand or effective tail-in packing.

Vazquez et al., 2014 rationalized the origin of this elevated TDS, including the dissolution of autochthonous (evaporite) or allochthonous (hydrologic emplacement) minerals such as halite, breach of proximal formations with elevated salinity, mobilization of hypersaline connate water, or combinations. Gdanski et al., 2007, showed the attributes of analyzing the ionic composition of flowback water to characterize the origin as formation or treatment water. Presuming the formation and treatment water are compositionally distinct, these authors coupled back-production forecasting with dissolution characterization and modeled the "movement of sodium, potassium, chloride, sulfate, carbohydrate, and boron during shut-in and production. As seen in Figure A-2, the computational requirements are to match the mass flow rate of the water and match the ionic composition of the produced fluid, with the final step being an assessment of the relative volume of recovered formation water and consequent

inference of fracture extent. Techniques such as these provide estimates of relative permeability and capillary pressure and first-order estimates of the productive fracture surface area.

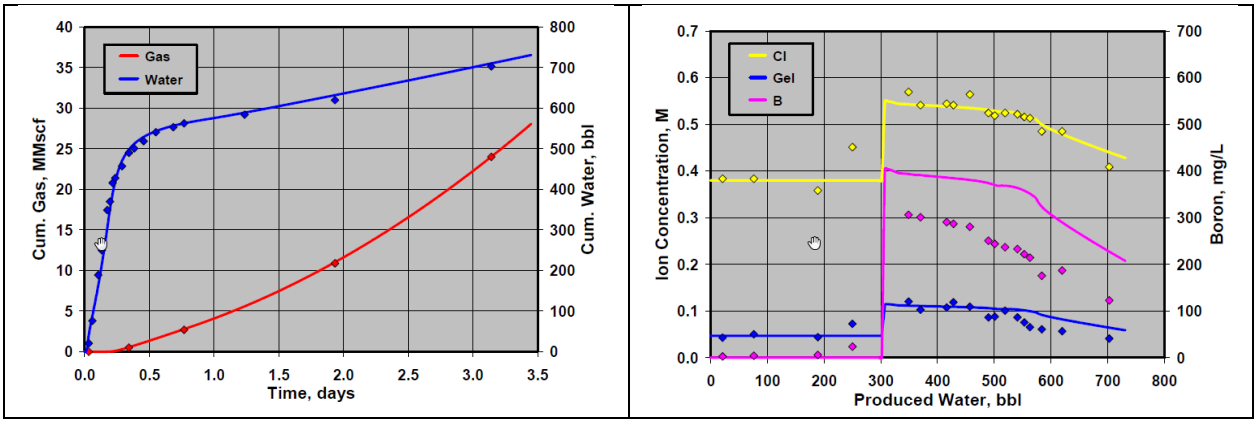

Figure A-2. At left, the first step is a basic history match of produced fluid from this well (Gdanski et al., 2007). With that comes a first-order assessment of fracture extent and reservoir properties. At right, the uniqueness of the forecast is improved by history matching produced species. In this case, there is returned gel, chlorides, and boron (crosslinker), as denoted in the legend. The discontinuity is likely due to an operational change such as increasing the choke size.

A clever analytical solution for evaluating flowback has been put forward by Zolfaghari et al., 2017. Recognizing that a plot of the salt concentration versus load recovery is commonly distinct among wells, these authors argued that the shape of this salinity profile could provide useful information about the created hydraulic fracturing network. Consider, three vertically separated productive formations in this play in northeastern British Columbia; Muskwa, Otter Park and Evie, each independently accessed by multistage horizontal well fracturing. Salinity data for flowback for these Horn River formation wells are shown in Figure A-3.

As can be seen in
Figure **A-3**, the salinity profiles for the Muskwa and Otter Park formations increase and then plateau. Returns from the Evie formation do not stabilize. The authors argued that early water with lower salt concentration comes from large aperture primary fractures. Logically, they reasoned that smaller aperture secondary fractures respond later. The consequence of this longer residence time is higher returned salinity, and the inference is a more complex fracture network. While geothermal scenarios are quite different, the relevance of monitoring flowed back or produced fluid seems reasonable.

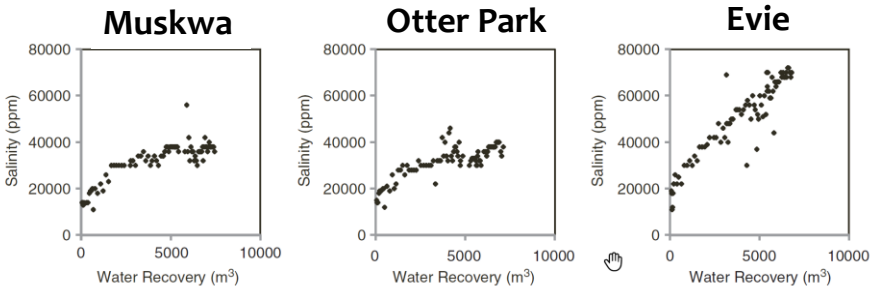

Figure A-3. Flowback salt concentration (expressed as salinity) versus the volume of water recovered for three vertically proximal Horn River producing formations after multistage stimulation of a horizontal well in each zone (Zolfaghari et al., 2017).

Zolfaghari et al., 2017 used a simple analytical model described schematically in Figure A-4. The logic is shown in the figure. A progressive increase in salinity (or an equivalent indicator) may indicate that the stimulated network is more complex, more dendritic. It is anticipated that early water recovered from hydraulically-generated fractures would come from fractures with larger apertures. Analytically, these authors rationalized the salt concentration to be low since the surface to volume ratio in these primary fractures would be expected to be lower than in the secondary fractures. As flowback proceeds, water from secondary fractures (with longer residence times) would be anticipated to be more saline.

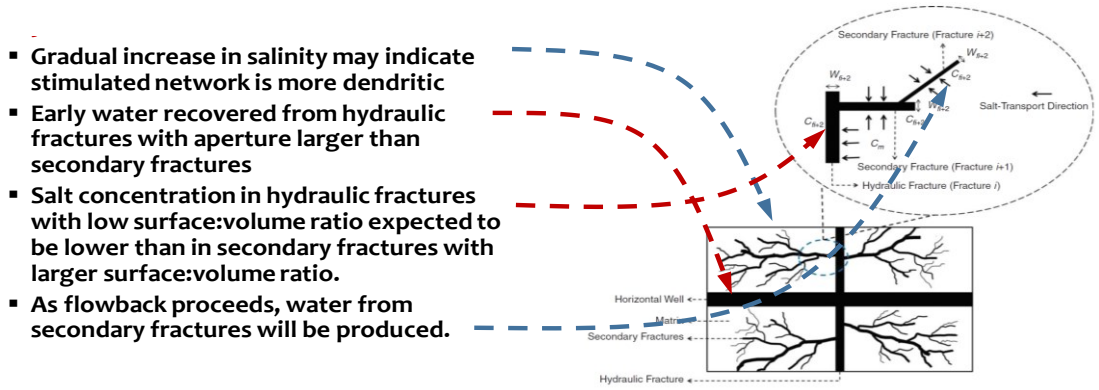

Figure A-4. Schematic of analytical model developed by Zolfaghari et al., 2017.

Presume that the salt travels from the matrix to the fracture by diffusion (Equation A-1).

$$J_i = 2DA_{f,i}\frac{C_m - C_{f,i}}{L_m} \approx 2DA_{f,i}\frac{C_m}{L_m} \tag{A-1}$$

where:

J ..... diffusion rate (kg/s),
$A_{f,i}$ ..... interfacial area between the matrix and the ith fracture (m^2),
D ..... diffusion coefficient (m^2/s),
C_m ..... salt concentration in the matrix (kg/m^3),
$C_{f,i}$ ..... salt concentration in the ith fracture (kg/m^3), and,
L_m ..... characteristic length (m)

and, with some assumptions and simplification, it can be seen that the concentration in an individual fracture is inversely proportional to its width, $W_{f,i}$ (Equation A-2).

$$C_{f,i}(W_{f,i}) = \frac{2DC_m\,\Delta t/L_m}{W_{f,i}} \tag{A-2}$$

Other authors have approached compositional and flowback analysis from a more traditional reservoir engineering perspective, trying to account mechanistically for what inhibits flowback (for example, Fei et al., 2016). Fei et al. presented a triple porosity (organic matter, inorganic matter, fracture network), dual permeability, chemical potential dominated water/gas flow model. Similarly, Bertoncello et al., 2014, provided some mechanistic rationalization for controlling flowback. They demonstrated that since increased liquid saturation near the fracture/formation interface in a tight gas reservoir profoundly impedes gas flow, extended shut-in before flowback can sometimes dramatically improve production. The tie to geothermal engineering is in the formal treatment of flowback from a reservoir engineering perspective.

The pressure transient reservoir engineering community has had a long-standing interest in flowback. Crafton, 1998, was one of the earliest proponents. His work showed the value of using the Reciprocal Productivity Index to estimate kh and stimulated surface area. The procedure could – at least qualitatively - provide information on effective or damaging flowback management strategies (effect of shut-ins, excessive drawdown …), and it enabled consideration of multistage completions. As time went on, there was increasing use of flowback analysis for horizontal wells. As an example, Deen et al., 2015, advocate using plots of the Reciprocal Productivity Index versus the square root of time. They referred to this as the Rate Normalized Pressure.

Xu et al., 2015, provide another example of flowback interpretation for early time gas production for a two-phase tank model (water-gas). These analyses will differ from many geothermal situations because they include drive mechanisms related to in situ gas or oil. Nevertheless, similar reservoir engineering concepts are relevant for flowback analysis in geothermal situations. These

types of analyses can legitimately be used to improve flowback procedures (Crafton, 2008; Crafton, 2010). Some of the early insight to analyses of this sort was provided by Ilk et al., 2010.

Other researchers have also developed predictions with boundary conditions consistent with these tank models (Clarkson, 2012). Some interpretations argue that early flowback data incorporates wellbore and fracture volume depletion (storage). Following on for this, Clarkson's group published on flowback analysis using rate normalized pressure and its derivative (Williams-Kovacs et al., 2012). Other similar publications have described simple models for multiply fractured horizontal wells. Abbasi et al., 2012, describe a well with a basic assumption similar to that described by Clarkson, 2012 - before putting well on flowback, induced fractures occupied by compressed fracturing fluid. This is a rate transient model with three flowback regions visible on diagnostic plots (water production, ramping up of hydrocarbons, hydrocarbon production). Figure A-5 is a schematic of this model. The simplification for enhanced geothermal reservoir engineering is that the drive for flowback does not include oil or gas and often little in situ water.

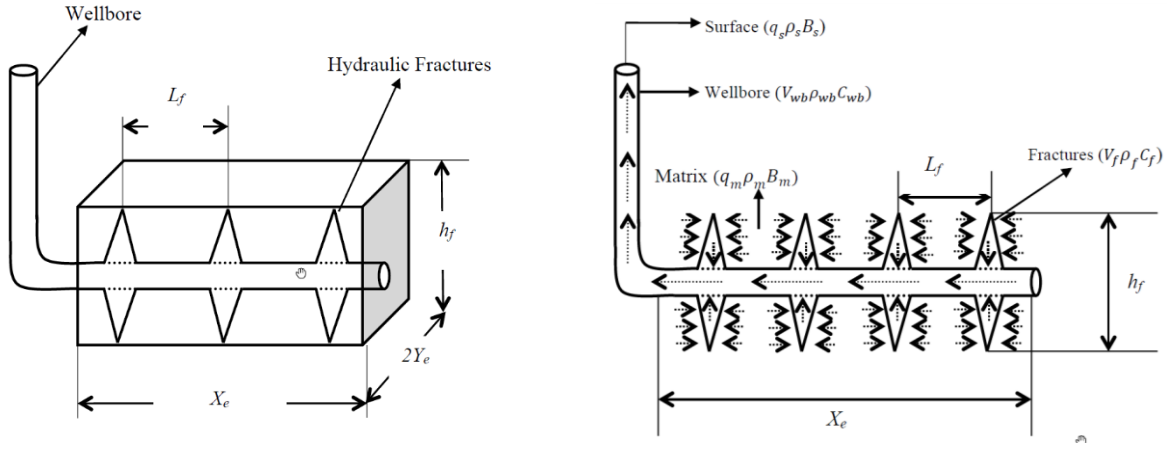

//

Figure A-5. Conceptual model for a multiply-fractured horizontal well developed by Abbasi et al., 2014.

The relationships governing the model are summarized below. Equation (A-3) shows the average pressure with time

$$\bar{P}(t) = P_{wf} + \frac{\phi_f C_t \mu}{K_f} \frac{(q_s - q_m)B}{2C_{st}} r_e^2 \left[\frac{1}{2}\ln\left(\frac{4A}{C_A \gamma r_w^2}\right)\right] \quad \text{(A-3)}$$

where:

P_{wf} ..... bottomhole flowing pressure,
ϕ_f ..... fracture porosity,
C_t ..... total compressibility,
μ ..... viscosity,
K_f ..... fracture permeability,
q_s ..... surface flow rate,
q_m ..... matrix flow rate,
C_{st} ..... total storage coefficient,
r_e ..... drainage radius,
A ..... drainage area of fracture,
c_A ..... Dietz shape factor for drainage area, and,
r_w ..... wellbore radius.

Of particular interest is the total storage coefficient. It includes the changes associated with fluid density and volumes of the fracture and the wellbore.

$$C_{st} = \frac{\mathrm{d}V_f}{\mathrm{d}P_f} + V_f C_f + V_{wb} C_{wb} \quad \text{(A-4)}$$

where:
V_f ..... fracture volume,
p_f ..... fluid pressure,
C_f ..... isothermal compressibility of fracture fluid,
V_{wb} ..... wellbore volume, and,
C_{wb} ..... isothermal compressibility of wellbore fluid.

Equation (A-5) expresses these relationships at the surface (as pressure normalized by surface rate

$$\frac{p_i - p_{wf}}{q_s} = \frac{N_P B}{q_s C_{st}} + \frac{\phi_f C_t \mu B}{2 C_{st} K_f} r_e^2 \left[\frac{1}{2} \ln\left(\frac{4A}{C_A \gamma r_w^2}\right)\right] \quad \text{(A-5)}$$

where:
B ..... formation volume factor (all fluids assumed equal), and,
P_i ..... reservoir pressure.

Finally, Equation (A-6) gives a rate normalized pressure. Its derivative with respect to the natural logarithm of time may also be relevant.

$$RNP = \frac{B}{C_{st}} MBT + \frac{\phi_f C_t \mu B}{2 C_{st} K_f} r_e^2 \left[\frac{1}{2} \ln\left(\frac{4A}{C_A \gamma r_w^2}\right)\right] \quad \text{(A-6)}$$

where:
RNP ..... rate normalized pressure, and,
MBT ..... material balance time (cumulative volume over instantaneous rate).

The workflow advocated by Abbasi et al., 2012, entails first evaluating the raw data, next plotting the RNP with time, and finally plotting the RNP with MBT. In the latter plot, referring to Equation (A-6), the slope and intersect will yield the total storage coefficient from which the fracture volume can be inferred. Geothermal applications will need to be modified but similar thinking could be relevant for flowback analysis.